Horizontal Dense-phase Pneumatic Conveying of Granular Material

I. Lecreps and K. Sommer, Germany

Abstract

By dense-phase conveying and particularly by slug-flow conveying, particles are conveyed in form of slugs partially filling the whole cross-section of a pipeline. This mode of flow needs only little gas to transport high capacities and minimizes product and pipeline damages. This paper studies first the applicability of a method developed by YI to predict the pressure drop by horizontal slug-flow pneumatic conveying. Experimental and predicted pressure drop show a good agreement for the materials tested. Based on the 3-layer-model of YI and WYPYCH describing dense-phase pneumatic conveying, operating points are depictured in a dimensionless state-diagram. In a second part, horizontal single slugs are investigated to determine the porosity and the stress states within a slug of cohensionless granular material. Thanks to a new measuring device including both stress and pressure sensors, wall shear stress, normal stress and pressure inside a slug could be determined simultaneously at different heights of the slugs. From pressure measurements, the slug porosity has been calculated and found to be higher than the bulk porosity itself. Both wall shear stress and normal stress are very high in comparison with values measured inside vertical slugs and behave differently according to the measurement position over the pipe cross-section.

Keywords: XXX??

1   Introduction

Pneumatic conveying of granular bulk solids is one of the most common and popular methods of industrial material transportation. By dense-phase conveying and particularly by slug-flow conveying, particles are conveyed in the form of slugs, which partially fill the complete cross-section of a pipeline. This mode of flow is gaining importance in industry because it needs only little gas to transport high capacities. Less product and pipeline damages, lower energy con-

sumption and smaller dust-separating requirements are further advantages.

In conveying granular materials, a transition regime between dilute-phase and dense-phase is observed (Fig. 1). Blockage, instability or even failure in conveying may take place in this transition region due to high pressure fluctuations resulting from the flow mode alteration between strand flow and slug flow. A lower pressure drop, however, can be achieved for operations close to its boundaries. Whereas the upper boundary of the transition zone has been a popular research topic, its lower boundary, i.e. the maximum conveying velocity of slug-flow conveying was rarely investigated.

Dilute-phase conveying has been studied in detail and is well understood but this is not the case for dense-phase conveying where current models provide different results [1-3]. In a
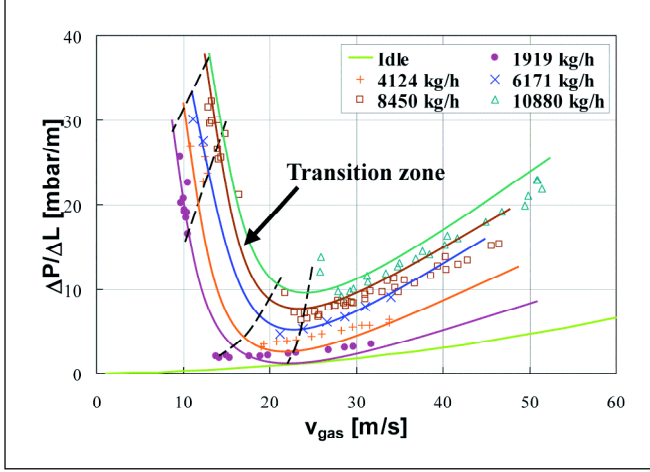
Isabelle Lecreps, Karl Sommer, Technische Universität München - Weihenstephan, Lehrstuhl für Maschinen- und Apparatekunde

Fig. 1: State-diagram for pneumatic conveying of Polypropylene-granules ($d_{equivalent}$ = 3.0 mm) through a 50 mm i.d. pipeline

recent article, SANCHEZ et al. [4] review models and correlations for dense-phase conveying and compare the various predicted results with their experiments, showing one more time the lack of precision of the models. For slug-flow conveying, the design of industrial plants is generally based on expensive tests on pilot plants, mostly in scale 1:1. Correlation of pressure loss, transport gas velocity and mass flow rate are generated each time for a specific material conveyed in a predetermined pilot plant. Pressure drop prediction by slug-flow conveying remains a problem and in practice, the risk of blockage in pipelines is usually minimized only empirically.

Recently, YI and WYPYCH [5] proposed a description for dense-phase pneumatic conveying and its boundaries based on a 3-layer-model. They also established a method to predict the pressure drop in a horizontal pipeline by slug-flow pneumatic conveying [6].

In the first part of this study, the pressure drop was measured along an 80 mm internal diameter pipeline and the results were compared with the pressure drop predicted from the method of YI and WYPYCH. In the second part, experiments involving a new measurement device including both stress and pressure sensors have been carried out to investigate simultaneously porosity and internal stress state of single slugs.

2 Theoretical Model

2.1 A 3-layer-model to Describe Dense-phase Conveying

When modelling horizontal pneumatic dense-phase conveying, the particular problem remaining is the expression of the porosity, which cannot be estimated as constant over the whole cross-section. Based on balances of mass, forces and momentum and on the unstable flow forming mechanism, WYPYCH und YI [5] established a theoretical 3-layer model for the prediction of the transition zone boundaries (Fig. 2). In the case of horizontal granular material conveying, they
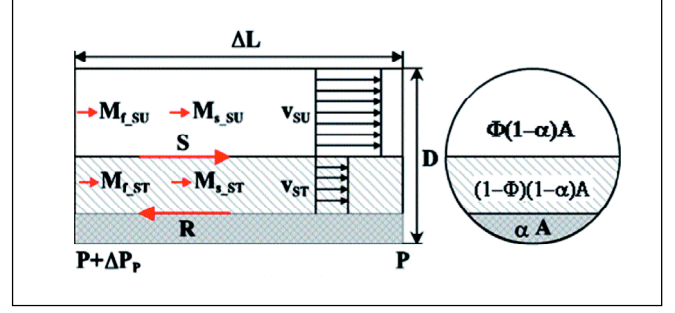

Fig. 2: 3-layer-model according to YI and WYPYCH [5]

identified a three-layer flow structure across the pipeline section: a suspension flow over a strand flow over a stationary layer or slowly moving bed. This model is an amelioration of the 2-layer-model of MOLERUS [7] and of WIRTH [8].

There are three basic assumptions for the establishment of the model: all the particles moving in the suspension above the strand are at the velocity of the air; all the particles moving in the strand are at the velocity of the air in the strand and the velocity of the slowly moving bed is negligible. From these hypotheses and from a combination of mass of air and solids balances, the following equation is obtained:

$$\frac{v_{st}}{v_{su}} = \frac{\phi}{1-\phi} \cdot \left[\frac{\rho_s \cdot (1-\varepsilon_{st})}{\rho_f \cdot \mu_{st}} - \varepsilon_{st} \right]^{-1} \quad (1)$$

The drive force results of the additional pressure gradient ΔP_p and of the shear stress S. From a force balance between shear force, additional pressure gradient and friction force R, the non-dimensional pressure drop ΔP can be presented as following:

$$\Delta P = \frac{\Delta P_p}{f_s \cdot \rho_s \cdot \left(1 - \frac{\rho_f}{\rho_s}\right) \cdot (1-\varepsilon_{st}) \cdot g \cdot \Delta L} = (1-\phi) \quad (2)$$

The shear stress acting on the interface strand/suspension is caused by the exchange of moving particles with different velocities. Through their impulse with the strand, particles of the suspension will be slowed down to the velocity of the strand. For each of these particles, a particle of the strand will be striped out and accelerated at the velocity of the suspension. From this assumption and from the combination of mass balance and force balance, the non-dimensional expression of the gas velocity can be defined as the friction number Fri:

$$Fri^2 = \frac{v^2}{f_s \cdot \frac{\rho_s}{\rho_f} \cdot \left(1 - \frac{\rho_f}{\rho_s}\right) \cdot (1-\varepsilon_{st}) \cdot D \cdot g} \quad (3)$$

From Eqs. (1)-(3), the picture of a diagram presenting dimensionless pressure drop versus friction number allows the definition of different regions corresponding to different flow types: steady-state strand flow, slug flow and unstable flow (Fig. 9).

2.2 Model for Pressure Drop Prediction of Horizontal Low Velocity Slug Flow

During slug-flow conveying, the movement of a single slug is balanced by a resistance force comprising three components: a friction force caused by the weight of the slug, a front stress caused by the stationary layer in front of the slug and a wall friction force caused by the lateral stress transmitted from the axial stress along the slug. Fig. 3 shows a slug element and the acting resistance forces.
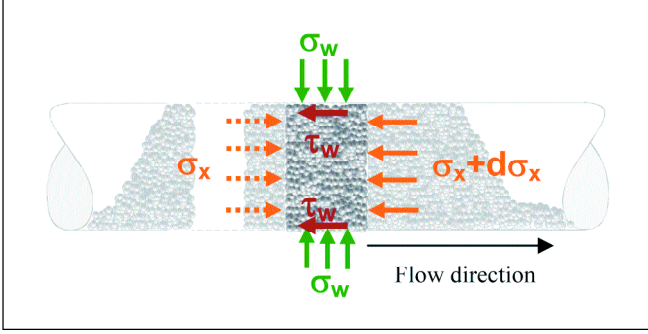

Fig. 3: Stresses acting on a horizontal moving slug

From this total resistance force for a moving slug providing Eq. (4) and with the help of the ERGUN equation (Eq. (5)), YI developed an iterative procedure to predict the pressure drop by horizontal slug flow [5].

$$\frac{\Delta P}{\Delta L} = \frac{4 f_w \cdot K_w}{D} \cdot \left[\left(\frac{\rho_s \cdot g}{K_w} \cdot H \right) + \alpha \cdot (1 - \alpha) \cdot \rho_s \cdot U_{slug}^2 \right] + $$
$$ + \rho_s \cdot f_w \cdot g \tag{4}$$

$$\frac{\Delta P}{\Delta L} = 150 \cdot \frac{(1-\varepsilon)^2 \cdot \eta \cdot U_{slip}}{\varepsilon^3 \cdot d_p^2} + 1.75 \cdot \frac{(1-\varepsilon) \cdot \rho_f \cdot U_{slip}^2}{\varepsilon^3 \cdot d_p} \tag{5}$$

2.3 Calculation of Stress Transmission Coefficient K_w

Eqs. (2), (3) and (4) are based on force and momentum balances and thereby involve either particle-particle friction factor fs or stress transmission coefficient K_w. The stress transmission coefficient is defined as the ratio of radial stress σ_r over axial stress σ_x:

$$K_w = \frac{\sigma_r}{\sigma_x} \tag{6}$$

These coefficients are difficult to determine experimentally and are mostly calculated from models.

Based on measurements of radial stress and calculations of axial stress, MI and WYPYCH [9] established a semi-empirical correlation between wall friction angle ϕ_w directly measured by means of a Jenike shear cell and particle-particle friction angle ϕ_s (Eq. (7)):

$$\phi_s = \frac{4}{3} \cdot \phi_w \cdot \gamma_b^{\frac{1}{3}} \tag{7}$$

$$\text{with } \gamma_b = \frac{\rho_b}{\rho_w} \tag{8}$$

where ρ_w is the density of water at 4 °C.

The particle-particle friction factor f_s is directly determined from the calculated angle ϕ_s (Eq. (9)):

$$f_s = \tan \phi_s \tag{9}$$

In their review, SANCHEZ et al. [4] show that the correlation of MI give good results when used to predict the pressure drop.

MI and WYPYCH [9] describe slug flow as an active stress case and give the following correlations:

$$\sin \omega = \frac{\sin \phi_w}{\sin \phi_s} \tag{10}$$

$$K_w = \frac{1 - \sin \phi_s \cdot \cos(\omega - \phi_w)}{1 + \sin \phi_s \cdot \cos(\omega - \phi_w)} \tag{11}$$

With the help of Eqs. (7)-(11), the stress transmission coefficient can be calculated from wall friction angle measurement.

2.4 Pressure Drop Prediction in Vertical Sections and Pipe Bends

The method of Yi and Wypych has been initially developed to predict the pressure drop in horizontal pipelines. To apply this method to vertical sections, a pressure drop to lift the solid mass has to be added. In pipe bends, a fictive length of pipe in dependence of pipeline diameter and bend radius is calculated [10].

3 Material and Methods

3.1 Physical Characteristics of Test Material and Conveying Equipment

Experiments were carried out in an 80 mm i.d. pilot plant with Polypropylene-granules (PP). Table 1 lists the main physical properties of the material tested. The wall friction angle ϕ_w has been determined by means of a Jenike shear cell TSG-70/140. Previous to the essays, granules were coated with the antistatic agent CIBA® Atmer® 129.

Experiments were carried out in an industrial scale pilot plant with a pipeline internal diameter of 80 mm. White Polypropylene pellets were conveyed along the 37 m pipeline by means of seven different air supplying velocities covering the

Table 1: Physical properties of materials tested

Test rig (i.d.)	Particle type	Mean size x_g [mm]	ρ_s [kg/m³]	ρ_b [kg/m³]	Porosity ε	Wall friction angle ϕ_w [°]	f_s	K_w
7 mm	glass	0.575	2487	1476	0.41	13.90	0.386	0.517
80 mm	Polypropylene (PP)	3.0*	889	553	0.38	9.69	0.187	0.816

* equivalent diameter

Table 2: Length of different sections of the i.d. 80 mm pipeline

| Section	Length horizontal [m]	Length vertical [m]	Length bend* [m]
1-2	5.08	-	-
2-3	2.00	-	-
3-4	-	3.24	8.96
4-5	1.15	3.60	8.96
5-6	12.05	-	-
1-6	20.28	6.84	17.93

* fictive length of bend

whole area of slug flow (from 3.7 to 4.8 m/s in conveying conditions). Six pressure transducers type Cerabar M Endress+Hauser, Germany allow the measurement of the total wall pressure at different points of the pipeline (Table 2). The test rig consists in two straight horizontal sections separated with a vertical section of 6.5 m height (Fig. 4).

3.2 Investigations on Single Slugs

3.2.1 Measurement Facilities

Investigations on single slugs have been carried out in the i.d. 80 mm industrial scale pilot plant (Fig. 4). At the end of the first horizontal conveying section where the flow has already

Fig. 4: Industrial scale pilot plant
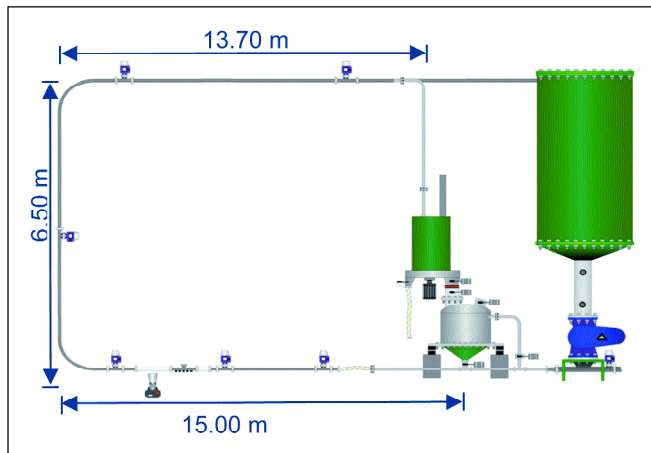
reached its stable state, a measurement stand has been integrated. To observe the type of flow, two short sections of the stainless steal pipeline have been replaced by two transparent PVC pipelines. Black particles were added to the white Polypropylene pellets in a ratio of 1/100 to play the role of tracers without changing the characteristics of the transported product. Thanks to a CCD camera that records the motion of tracer particles transported by a slug and with the assumption that the particles velocity in the middle of a slug is equal to the velocity of the slug itself, the latter one can be determined.

A special measurement device has been developed to allow the measurement of pressure, wall shear stress and normal stress within a slug at the same time without disturbing the conveying (Fig. 5). A short section of the pipeline has been instrumented with both pressure and force sensors and has been rotated for the different essays (Fig. 6). Six miniature pressure sensors type XTM-190M, Kulite Semiconductor Products Inc., New Jersey, measure the pressure inside a slug each 3 cm. Two piezoelectric force sensors type 208C01 PCB, Piezotronics Inc., USA, are connected to a measurement plate, which simulates a piece of the pipeline wall. Thanks to their perpendicular arrangement, the force sensors enable the simultaneous detection of wall shear stress and normal stress within a slug.

Signals of all pressure, force and temperature sensors are amplified and transformed in a 16 bit signal by means of a DAQ board. All signals are finally treated in the program LabView 5.1.

At first, the piezoelectric force sensors have to be calibrated. For this purpose, two masses of 50 and 100 g, resp., are successively used to stress each sensor individually in axial or radial direction. Measurements show a linear dependence between stress and output signal. However, interdependence exists between axial and radial signals due to the perpendicular arrangement of the force sensors. This linear interdependence is calibrated and corrected.

Other factors have also an effect on the force measurement. For a constant stress, the force sensors show a discharge with the time in form of an exponential function. The exponential function coefficients are determined and used to correct the output signal. Secondly, the piezoelectric sensors display a high dependence on temperature. To avoid temperature fluctuations, the calibration is carried out in a climatic chamber. Moreover, a NTC-thermocouple placed directly in the measurement chamber enables a sensitive control of the temperature.

Conveying occurs by overpressure in the pipeline system. The force sensors will detect this overpressure as a stress. To avoid this interaction, small holes assure the pressure equilibrium between conveying section and measurement cham-
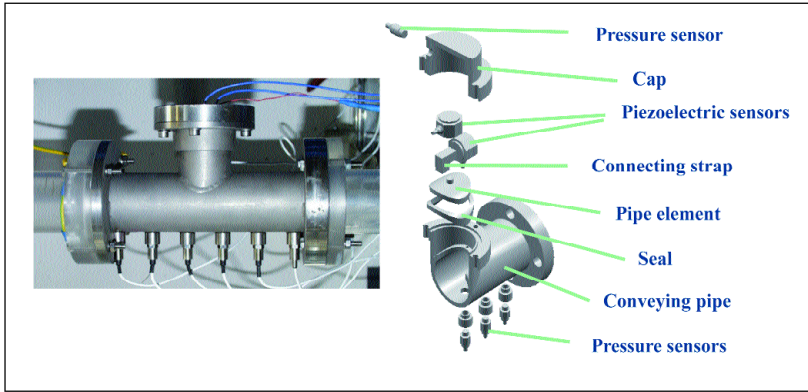
Fig. 5: Picture and schematic construction of the probe for the simultaneous detection of wall shear stress, normal stress and pressure inside a slug
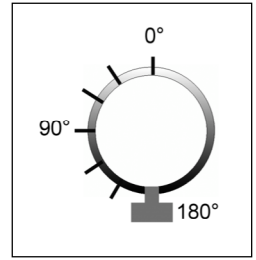

Fig. 6: Different positions of the measurement plate to detect both stresses over the whole pipeline cross-section

3. By means of a CCD camera and tracers particles, the slug velocity is determined.

4. The relative velocity between gas and slug is calculated.

ber. Furthermore, before the essays the piezoelectric elements are submitted to various environmental pressures to calibrate their pressure sensitivity. During conveying, a miniature pressure sensor placed in the measurement chamber detects the remaining pressure difference between conveying pipe and measurement chamber and enables the corresponding correction of the output signal.

After calibration of these interaction factors, the computer delivers two pure signals for the wall shear stress and the normal stress within a slug.

3.2.2 Measurement of Both Axial and Normal Stresses

In the literature, it is always presumed that a porosity gradient takes place across the section of a slug: due to the gravity effect, the slug density is estimated higher at the bottom than in the upper part of a slug.

To be able to verify this assumption by means of experimental investigations, the instrumented probe has been rotated for the various essays so that the measurement plate was successively located at different angles of the pipe cross-section.

As shown in Fig. 6, seven positions have been tested to detect both the stresses over the whole pipeline circumference: 0° when the measurement plate is located above, 180° when it is located below and five other positions with 30° between them.

3.2.3 Determination of Slug Porosity

The determination of the slug porosity is indirect and results from pressure measurements. The method, presented in Fig. 7, consists of several steps:

1. The pressure loss between two miniature pressure sensors is calculated from local pressure measurements. In this interval of few centimetres, gas expansion can be considered as negligible.

2. The velocity of the gas supply is known for atmospheric conditions. This velocity will be converted to the pressure conditions in the measurement area.

5. The pressure loss between two miniature pressure sensors and the relative velocity are finally inserted in the ERGUN equation (Eq. 5) which provides the relative slug porosity.

4 Results and Discussion

4.1 Pressure Loss

To describe the occurring two-phase flow, it is necessary to know experimental parameters as granules characteristics, pipeline properties or air velocity and to measure the solids mass flow rate and the pressure drop along the pipeline. Following the method of Yi and Wypych, the pressure drop along the pipeline could be predicted and compared with the experimental pressure drop directly measured by two pressure transducers.
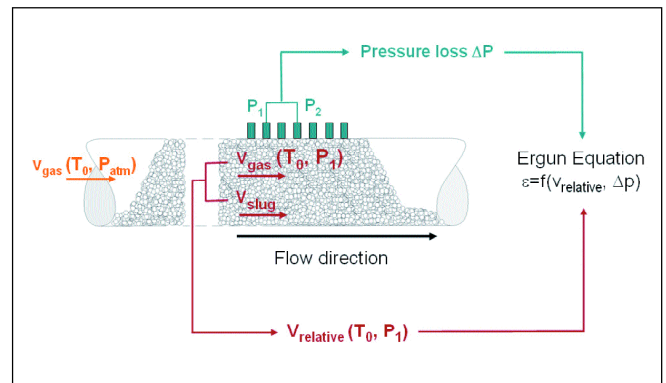

Fig. 7: Indirect method for the determination of the slug porosity

Fig. 8 compares both experimental and predicted pressure drop for different sections of the pipeline (see also Fig. 4). The error indexes on the predicted results in Fig. 8 represent the field ± 25% of the predicted value in which agreement is considered as good. The method bases on balances for a slug moving in a horizontal pipeline.

For vertical and bends sections, an additional pressure loss have been taken into account as mentioned previously. The sections properties are summarised in Table 2.
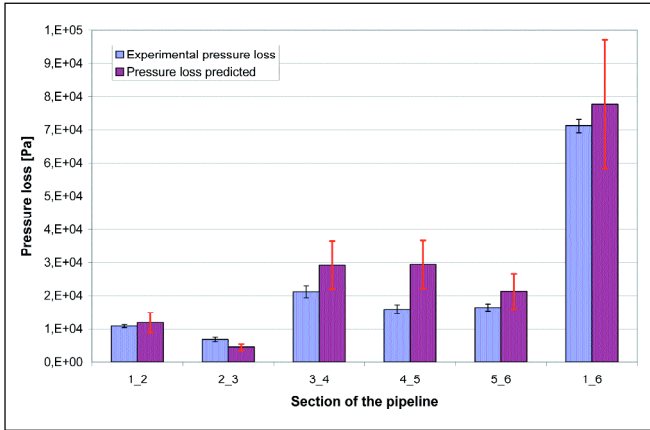
Fig. 8:   Experimental and predicted pressure drops for different sections of the 80 mm i.d. pipeline system

The best agreements are obtained for the first horizontal section 1-2 and for the whole pipeline system 1-6 with a difference between experimental and predicted results of 9% in each case. The poorer agreements are obtained for the two sections 3-4 and 4-5 including each time a bend for which a fictive length has been taken into account.

4.2   Dimensionless State-diagram

Fig. 9 shows the depicting of the dense-phase boundaries and the calculated operating points for PP-granules obtained for six essays. For these essays, the material has been transported with the minimum gas velocity necessary for the slugs to move without blockage of the system. Calculated operating points are located in the slug flow region and display a very high pressure loss.

A dimensionless state-diagram allows the direct comparison of operating points for different conveying rigs and products.

4.3   Porosity within Horizontal Slugs

Following the indirect method presented in Fig. 7, the porosity within horizontal slugs conveyed through 80 mm i.d.

Fig. 9:   Depicting of the operating points for PP-granules conveyed with the minimum air supply velocity
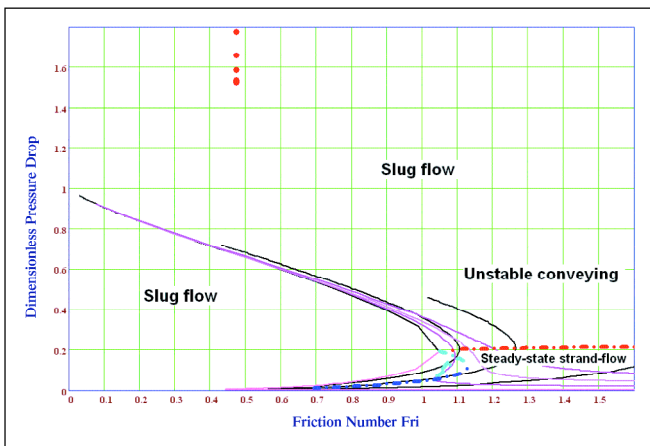
pipeline has been determined from pressure measurement. Even if the miniature pressure sensors were located at various positions over the pipeline cross-section for the different experiments, gas physics implicates that pressure is the same over this whole cross-section. It is therefore not possible to measure pressure differences over the pipeline cross-section and therewith porosity differences over the whole height of a slug.

Pressure is measured with a frequency of 100 Hz. Therefore, 100 porosity values are obtained per second. These values are named "relative porosity" because they do not describe the mean slug porosity between its front and its back but over the whole cross section for a given point along the slug.

Fig. 10 shows the calculated porosity for slugs obtained with four of the seven different air supply velocities tested under which the minimum and the maximum velocities. To make the representation clearer, negative pressure losses due to measuring errors of the sensors themselves have been replaced by the value 0, generating a porosity of 1.

The relative porosity remains constant over the whole length of a slug if we exclude its front and back. For these two sections, it should be noted that the porosity is an average over the whole cross-section, even if the material fills only a part of this cross-section.

For all slugs analysed, the porosity over the cross-section is located between 0.6 and 0.7. Slug porosity is therefore higher than the porosity of the bulk solids itself ($\varepsilon = 0.38$). When the velocity of the air supply is increased, slugs move faster and become shorter. Nevertheless, slug porosity still displays the same values as illustrated in Fig. 10.

Slugs appear fluidised. However, since the porosity determination bases on pressure measurement, it is not possible to distinguish if slugs are homogeneously fluidised or if they display a porosity gradient over the pipeline cross-section i.e. over the slug height. The notion of porosity gradient is frequently mentioned in the literature and recently by YI and WYPYCH in their 3-layer-model (see Fig. 2).

4.4   Radial and Wall Shear Stress within Horizontal Slugs

4.4.1   Typical Aspect of Curves Detected by the Probe

The measurement device including both stress and pressure sensors provides characteristic curves according to the position of the measurement plate over the pipeline circumference. Typical curves are presented in Figs. 11a - 11c.

These curves show three waves corresponding to three slugs which passed through the instrumented pipeline section in a time lap of respectively 10s, 8s and 15s ($v_{air} = 3.7$ m/s). The run of the radial stress curve shows at best when a slug arrives in the measurement zone and then goes further. The pressure curves show this characteristically run too but in
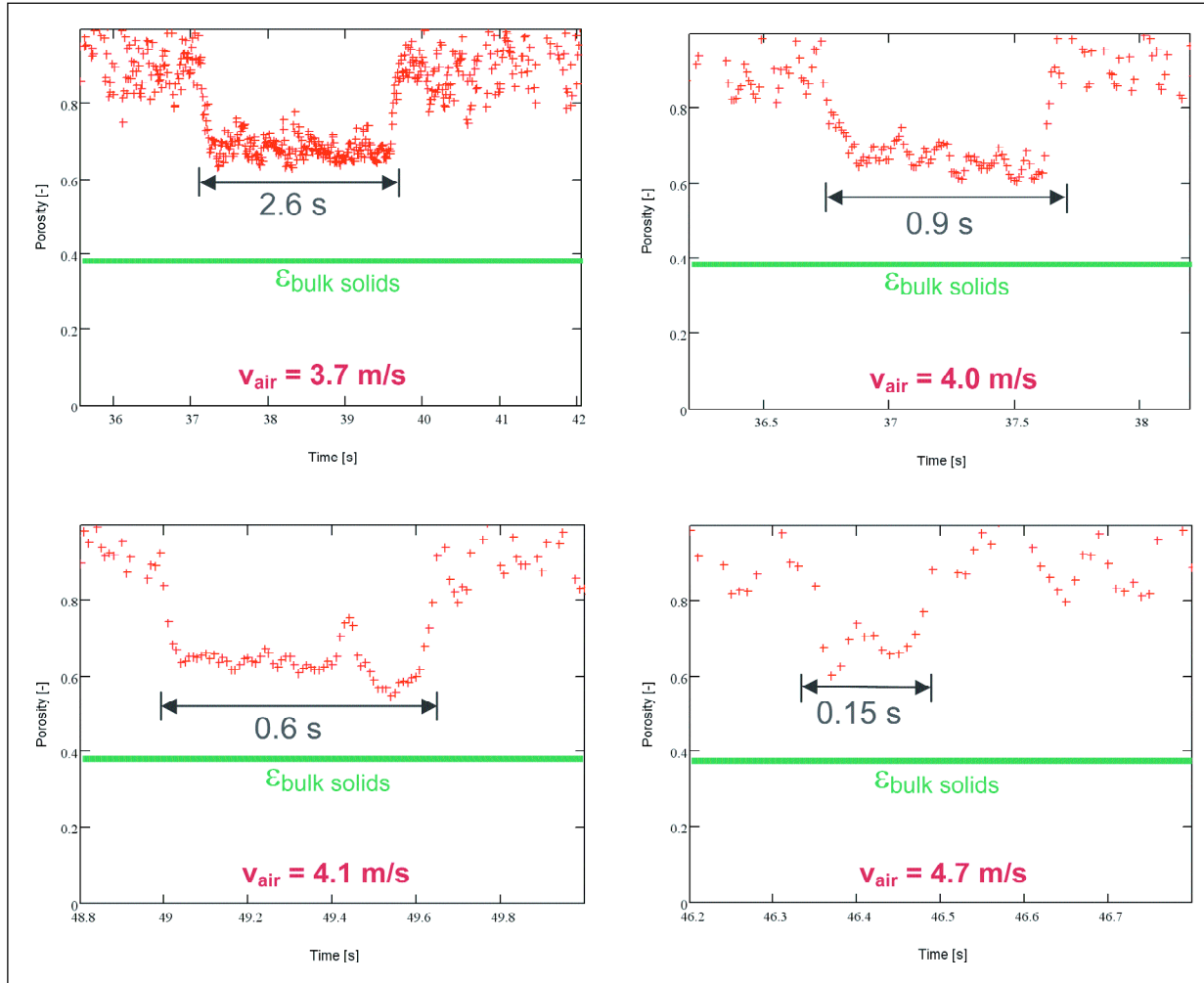
Fig. 10: Calculated porosity within four horizontal slugs conveyed with air supply velocities between 3.7 m/s and 4.7 m/s.

this case, pressure picks are observed. Indeed, when a slug has just passed through the instrumented pipeline section, there remains an overpressure that disappears slowly.

The radial stress, however, if transmitted from axial stress, should exist only inside a slug and therefore should be only detected if a part of the slug is just located in the measurement plate zone. Radial stress was found to remain nearly constant over the whole length of a slug, except at its front and back. For all measurement positions and each slug detected, the increase of radial stress and pressure occurs simultaneously.

Pressure

The weight of granules deposited on the measurement plate is detected as normal stress as well. When the measurement plate is placed at the bottom (180° in Fig. 6), the stress due to the weight of particles reaches a maximum and has been evaluated to 290 Pa. This value represents less than 3% of the normal stress average and can hence be considered as negligible.

It should be noted that stress values are sometimes smaller than zero. This effect due to the sensors calibration has been corrected for numerical analysis.

441 slugs were analysed as single slugs. According to the measurement position, different aspects of stress curves are observed. For upper positions, when the measurement plate is placed between 0° and 120° (Fig. 6), curves for radial and wall shear stress are perfectly in phase: both curves reach their minimum and maximum at the same time and show very similar runs (Fig. 11a). When the measurement plate is positioned at 150°, which means almost at the pipeline bottom, wall shear stress curves present the same aspect as radial stress curves but are slightly delayed (Fig. 11b). Finally, when the stresses are measured at the pipeline bottom, radial and wall shear stress curves are out of phase: a curve reaches its maximum when the other one is very low and reciprocally (Fig. 11c).

At the pipeline bottom, between two slugs, there remains a layer of particles that have been just deposited by a slug and are going to be picked up by the next one. For a defined product and pipeline system, the height of the deposited layer depends on the conveying velocity. For a decreasing gas velocity, the height of this layer increases until blockage occurs because the conveying force does not suffice anymore to transport slugs further.

According to Fig. 11a-11c, two phenomena have to be distinguished: in the upper part of pipeline, the highest wall
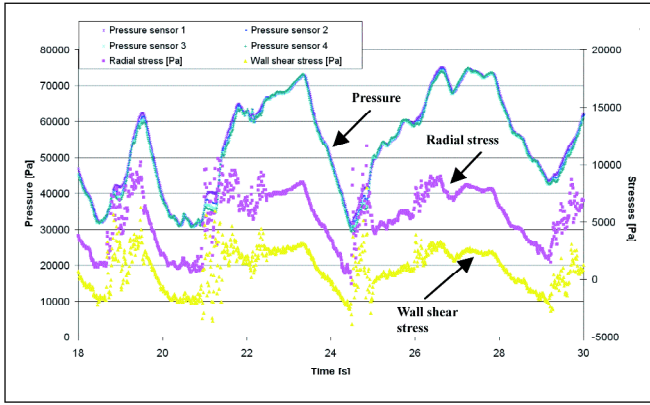
Fig. 11a: Typical curves provided by pressure and stress sensors placed between 0° and 120°
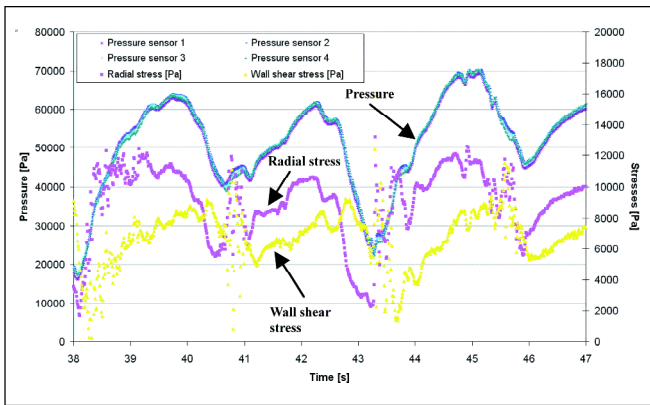

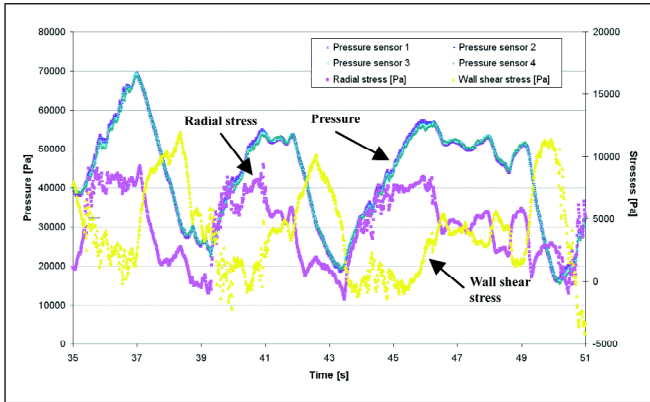Fig. 11b: Typical curves provided by pressure and stress sensors placed at the position 150°

Fig. 11c: Typical curves provided by pressure and stress sensors placed at the bottom (position 180°)

shear stress values are detected within slugs. At the bottom of the pipeline, they are detected after the passage of a slug, when only a layer of deposited particles remains.

4.4.2 Radial and Wall Shear Stresses

Radial and wall shear stresses behave differently according to the measurement position at the pipeline circumference. Basically, three diferent behaviours can be distinguished: at the top of the pipeline, at the bottom and between these two borders (positions 30° to 120°). Each stress value presented

is a mean calculated for nine slugs issued during three conveying tests carried out at the same conditions. Values are read when the respective stress reaches its maximum, one stress pick or plateau corresponding to one slug.

At the top of the slugs: The radial and wall shear stress curves are in phase. The maximum wall shear stress values are therefore detected within slugs. Both stresses depend strongly on the conveying air velocity: they increase with the increase of the velocity. Between the lower and the upper slug-flow boundaries, both stresses are doubled (Fig. 12).
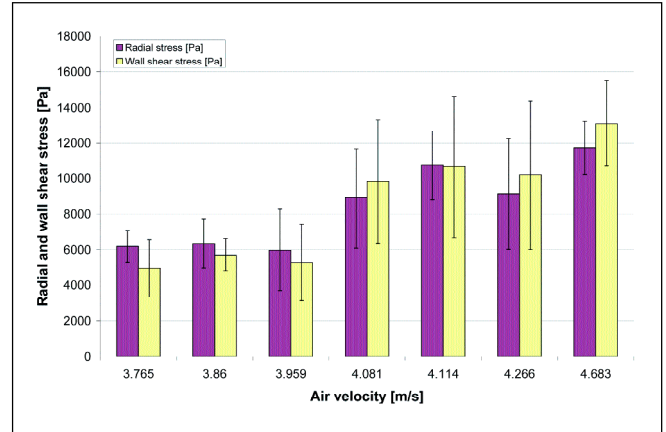

Fig. 12: Stresses detected at the top of the slugs

In the bottom part of the slugs: The radial and wall shear stresses are out of phase. The wall shear stress picks are detected respectively behind each slug. Fig. 13 shows that wall shear stress depends highly on the conveying air velocity and reaches very high values (15000 Pa) near the upper boundary of slug-flow. In contrast, radial stress is not sensitive to the increase in velocity and displays constant values of some 8500 Pa.
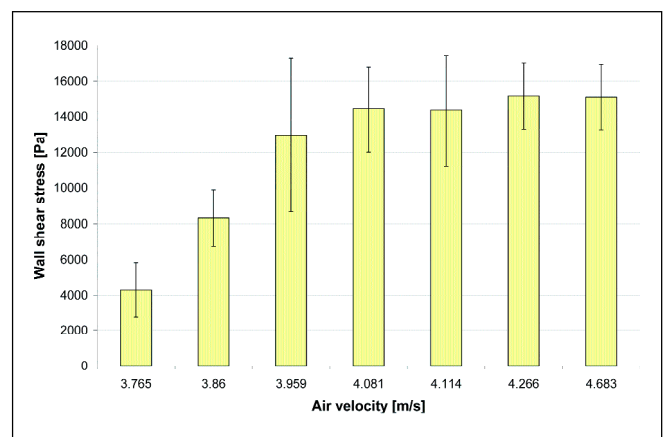

Fig. 13: Maximum wall shear stress detected at the bottom (between two slugs

At intermediate positions: Just as in the top part of the slugs, radial and wall shear stresses are in phase, i.e. wall shear stress picks are detected within slugs. However, contrary to the top position, both stresses do not depend on the air velocity. For all intermediate positions, values are about 4500 Pa

Table 3: Radial and wall shear stress according to the situation over the pipeline circumference

Position		Top ⌀ 0°	Intermediate 30° to 120°	Bottom ⌀ 180°
Radial stress	Velocity dependence Amplitude	Yes from 6000 to 11500 Pa	No 7000 Pa ± 15%	No 8500 Pa ± 20%
Wall shear stress	Max. detected Velocity dependence Amplitude	within slugs Yes from 5000 to 13000 Pa	within slugs No 4500 Pa ± 15%	between slugs Yes from 4000 to 15000

± 15% for radial stress and 7000 Pa ± 15% for wall shear stress.

It has been always supposed that porosity gradient exists within the cross-section of a slug, i.e. that slug density is higher at the bottom that above. In this case, the normal stress, if transmitted from axial stress, should show some significant differences according to the situation over the cross-pipeline. Since no significant difference could be noted between stresses measured in the upper and in the lower part of slugs, this hypothesis cannot be validated here. Nevertheless, the radial stress shows a tendency to be higher in the upper part of slug. However, differences are significant only for the lowest air velocities.

Stresses measured inside horizontal slugs are much higher than stresses measured during previous studies inside vertical slugs [12]. The radial and wall shear stresses were respectively about 1500 Pa and 750 Pa inside vertical slugs conveyed with the minimum supplying air velocity.

Results referring to radial and wall shear stresses are compiled in Table 3.

4.5 Concluding Remarks

It does not matter how fast a slug of granular material (as investigated in this study) moves, its porosity is always the same. All 441 slugs of plastic pellets examined displayed a relative porosity in the range of 0.6 – 0.7.

However, the method used for the porosity determination does not allow us to identify if slugs are homogeneously fluidised or if they display a gradient of porosity over their height.

Nevertheless, radial stress displays high values over the whole pipeline cross-section. If slugs are fluidised over their whole length, they cannot be considered as compact bulk solids structures. In this case, it is expected that radial stress cannot be transmitted from axial stress. Another phenomenon has to be responsible for the high radial stress values recorded.

At the top of the slugs, both radial and wall shear stresses increase significantly with the increase of the air supply velocity. However, it is not the case in the lower layers. This effect may be connected to the presence of a thin layer of air free of particle at the top of the pipeline and so at the top of the slugs. This phenomenon is usually observed in industries using pipeline diameters bigger than 200 mm.

Immediately after the passage of each slug, when only a thin layer of particles remains at the bottom, a pick of high wall shear stress was detected. Further investigations taking into consideration the kinetic theory of gases will demonstrate if all these high stress values are due to the stochastic agitation of particles. In this case, stresses would be proportional to the number of impacts between particles and wall on the one hand and to the air velocity on the other hand.

To understand the full mean of these results, it is important to keep in mind that the hydrostatic pressure due to the weight of a slug is negligible and that the overpressure prevailing in the pipeline does not appear in the stress results.

4.6 Influence of f_s and K_w on the Predicted Pressure Drop

Values of particle-particle friction factor f_s and values of stress transmission coefficient K_w have been calculated from the MI and WYPYCH correlation. This correlation is based on the measurement of normal stress and calculations of axial stress.

Thanks to the measurement device presented in this study, it is possible to determine values of K_w based only on experimental investigations. For this purpose, values of radial stress are directly obtained from normal stress measurement and values of axial stress are obtained from wall shear stress measurements after transformation with the help of the Mohr's circle.

Values of K_w and f_s are very important for the prediction of pressure drop. Fig. 14 shows the very good agreement between experimental and predicted pressure drop for glass granules (Table 1) conveyed in a 7 mm i.d. pipeline after
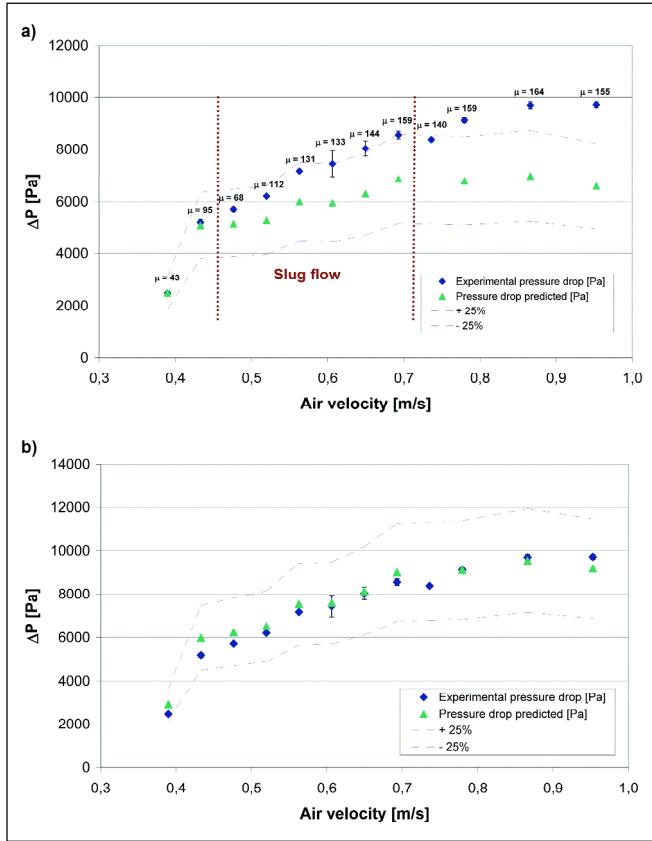
Fig. 14: Agreement between experimental and predicted pressure drop for glass granules conveyed in i.d.7 mm pipeline;   a) $K_w = 0.517$; b) $K_w = 1$)

recalculation with a K_w value of 1 ($K_w = 0.517$ in Table 1 (calculated from the MI and WYPYCH correlation)).

In addition, calculations of K_w based on experimental investigations only will permit to verify if this parameter describes effectively a transmission of stress from the axial to the radial direction.

5   Conclusion

Dense-phase pneumatic conveying is gaining importance in industry for the transportation of granular material. But the complexity of the laws governing this mode of transport makes it difficult to understand and to predict it. The models already existing employ different approaches and give very different results. In industry, the design of dense-phase systems remains mainly empiric.

To check the applicability of the YI method to predict the pressure drop by horizontal slug flow pneumatic conveying, experiments were carried out in pipelines of 7 mm (results only partially presented) and 80 mm internal diameter. Experimental and predicted pressure drop show a good agreement for the materials tested.

By means of the YI and WYPYCH 3-layer-model, which describes low-velocity dense-phase conveying, the operating points for experiments conducted near the lower boundary of slug flow could be calculated and depicted on a dimension-

less state-diagram. The operating points were effectively located in the slug-flow area.

Investigations on single slugs conveyed in an 80 mm i.d. pipeline permitted to learn more about stress state and porosity within a slug of cohesionless granular material.

With the help of the ERGUN equation and pressure loss measurements, the slug porosity could be indirectly determined. The porosity remains constant over the whole length of a slug (except at its front and back) and displays values in the range of 0.6 – 0.7 for slugs generated in the whole area of slug-flow. The slug porosity is therefore higher than the bulk solids porosity itself ($\varepsilon = 0.38$). A slug-catcher is currently developed to investigate more precisely the fluidization state of the slugs. This device is able to catch a moving slug and separate it simultaneously in three horizontal layers so that a potential porosity gradient over the height of a slug can be detected.

Radial and wall shear stresses behave differently according to the measurement position over the pipeline circumference. High radial stresses were detected over the whole cross-section. Since slugs are fluidised, the radial stress cannot be explained by the stress transmission issued from the axial stress.

The stochastic agitation of the particles may be the cause for the high radial and wall shear stresses recorded at the top of each slugs and for the high wall shear stress recorded between slugs at the bottom of the pipeline.

Values of K_w and f_s have a big influence on the result of predicted pressure drop. The semi-empirical correlation of MI and WYPYCH that is used in this study to calculate K_w and f_s from ϕ_w measurement should be verified by means of K_w calculations resulting only from experimental investigations. The measurement device presented in this study enables the simultaneous measurement of both normal and wall shear stresses and thereby the experimental determination of K_w by means of Mohr's circle.

All this aim to describe and to understand the comportment of single slugs in order to validate or to adapt models that were already proposed for the prediction of the pressure drop by slug-flow pneumatic conveying on the one hand and for the prediction of the flow type on the other hand.

Nomenclature

d_p	particle diameter	[m]
D	pipe internal diameter	[m]
f_s	particle-particle friction factor	[-]
f_w	particle wall friction factor	[-]
g	gravitational acceleration	[m/s^2]
H	height of the suspension over the strand	[m]

K_{w}	stress transmission coefficient	[-]
ΔL	elemental length	[m]
ΔP	pressure difference	[Pa]
ΔP_{p}	pressure drop due to particles	[Pa]
U_{slip}	superficial slip velocity	[m/s]
U_{slug}	slug velocity	[m/s]

Greek letters

α	relative area of stationary bed	
γ_{b}	bulk specific gravity with respect to water at 4 °C	
ε	voidage	[-]
η	viscosity	[Pa·s]
μ	solids loading	[-]
ν	air velocity	[m/s]
$\rho_{\mathrm{f}}, \rho_{\mathrm{s}}$	air, particle density	[kg/m^3]
ρ_{b}	bulk density	[kg/m^3]
$\sigma_{\mathrm{x}}, \sigma_{\mathrm{r}}$	axial, radial stress of particle slug	[Pa]
σ_{w}	normal stress	[Pa]
τ_{w}	wall shear stress	[Pa]
ϕ	fraction of cross-sectional area not occupied by strand and stationary bed	[-]
ϕ_{w}	wall friction angle	[°]
ϕ_{s}	static internal friction angle	[°]

Subsripts

| st | strand section |
| su | suspension section |

References

[1] KONRAD, K., D. HARRISON, R.M. NEDDERMAN, and J.F. DAVIDSON: Prediction of the pressure drop for horizontal dense phase pneumatic conveying of particles; Pneumo-transport 5, London, UK (1980), pp. 225-244.

[2] MI, B., and P.W. WYPYCH: Pressure drop and slug velocity in low-velocity pneumatic conveying of bulk solids; Powder Technology 94 (1997), pp. 123-132.

[3] MUSCHELKNAUTZ, E., and W. KRAMBROCK: Vereinfachte Berechnung horizontaler pneumatischer Förderleitungen bei hoher Gutbeladung mit feinkörnigen Produkten; Chem.-Ing. Tech. 41 (1969) No. 21, pp. 1164-1172.

[4] SANCHEZ, L., N.A. VASQUEZ, G.E. KLINZING, and S. DHODAPKAR: Evaluation of models and correlations for pressure drop estimation in dense phase pneumatic conveying and an experimental analysis; Powder Technology 153 (2005), pp. 142-147.

[5] WYPYCH, P.W., and J. YI: Minimum transport boundary for horizontal dense-phase pneumatic conveying of granular materials; Powder Technology 129 (2003), pp. 111-121.

[6] YI, J.: Transport boundaries for pneumatic conveying; PhD thesis, University of Wollongong (2001).

[7] MOLERUS, O.: Fluid-Feststoff-Strömung – Strömungsverhalten feststoffbeladener Fluide und kohäsiver Schüttgüter; Springer Verlag, Berlin (1982), pp. 134-156.

[8] WIRTH, K.E.: Theoretische und experimentelle Bestimmungen von Zusatzdruckverlust und Stopfgrenze bei pneumatischer Strähnenförderung; PhD Thesis, Universität Erlangen-Nürnberg, Germany (1980).

[9] MI, B., and P.W. WYPYCH: Investigations into wall pressure during slug-flow pneumatic conveying; Powder Technology 84 (1995), pp. 91-98.

[10] FLATT, W.: Grundbuch für die pneumatisch Förderung; Gebrüder Bühler AG, Uzwil, Switzerland (1975).

[11] LAOUAR, S.: Etude du transport pneumatique dense aux très basses vitesses; PhD Thesis, Technical University of Compiègne, France (1995).

[12] NIEDERREITER, G.: Untersuchung zur Pfropfenenstehung und Pfropfenstabilität bei der pneumatischen Dichtstromförderung – Experiment und mathematische Modellierung; PhD Thesis, Technical University of Munich, Germany (2006)